RESEARCH ARTICLE

Special Section:

Key Points:
- Devices to manipulate and control electromagnetic surface waves
- Generic modeling and design method by combining graded-index materials and transformation optics theory
- The approach can be used for the manufacturing of new cloaking devices

Supporting Information:
- Supporting Information S1

Correspondence to:
Y. Hao,
y.hao@qmul.ac.uk

Modeling and design for electromagnetic surface wave devices

Luigi La Spada[1] [ID], **Sajad Haq[2]**, and **Yang Hao[1]**

[1]School of Electronic Engineering and Computer Science, Queen Mary University of London, London, UK, [2]QinetiQ Ltd, Farnborough, UK

Abstract A great deal of interest has reemerged recently in the study of surface waves. The possibility to control and manipulate electromagnetic wave propagations at will opens many new research areas and leads to lots of novel applications in engineering. In this paper, we will present a comprehensive modeling and design approach for surface wave cloaks, based on graded-refractive-index materials and the theory of transformation optics. It can be also applied to any other forms of surface wave manipulation, in terms of amplitude and phase. In this paper, we will present a general method to illustrate how this can be achieved from modeling to the final design. The proposed approach is validated to be versatile and allows ease in manufacturing, thereby demonstrating great potential for practical applications.

Plain Language Summary There is a crucial interest in exploring electromagnetic waves traveling on materials surface. The study and manipulation of such waves is the key to develop technological and industrial solutions to reduce and mitigate important issues in the design of real-life platforms, for different application fields, ranging from microwave to optics. We propose a general theory for designing perfect surface wave cloaks; such a theory creates a robust link between truly arbitrary surfaces and their analogue material properties in an intuitive manner. Most importantly, with slight modifications, the underlying theory can be applied to other physical phenomena that are described via wave equations.

1. Introduction

Surface waves typically exist at the interface between two different media, for any flat or curved stratified structures [*Polo et al.*, 2013]. Electromagnetic waves can propagate as surface waves if they can be "guided" along a refractive index gradient material or an interface between two media having different dielectric constants [*Hill and Wait*, 1978]. In mechanics, a common example of surface wave is gravity wave propagating along the surface of liquids (i.e., ocean waves). Gravity waves [*Gill*, 1982] can also occur within liquids, at the interface between two fluids with different densities. Elastic surface waves can travel along the surface of solids, with an amplitude that typically decays exponentially with depth into the substrate: typical examples are the Love [*Love*, 1911], Rayleigh [*Viktorov*, 2013], and surface acoustic waves [*Oliner*, 1978].

Despite all the different types of surface waves, they are widely used in many practical applications. For electromagnetic surface waves, their characteristic of being acutely sensitive to any variation of the refractive index represents the basis for high-Q sensors [*Iovine et al.*, 2014]. Moreover, their use in enhancing light absorption of photovoltaic solar cells gained huge attention and many techniques to increase the efficiency of light harvesting have been investigated [*La Spada and Vegni*, 2016]. Applications of surface waves are also in communications [*Vegni and Loscrì*, 2016]: their use in optical technology can reduce dissipation and promoting short-, as well as, long-range communications, bringing the advantages realized with optical fibers to the nanoscale.

One of the most recent and popular application is the design of invisibility cloaks, which is used to effectively render the object invisible from impinging electromagnetic waves. Several approaches have been proposed over the years to accomplish this aim, ranging from the classical scattering cancellation approach [*Chen et al.*, 2012] to other well-established technologies based on the use of frequency selective surfaces [*Munk*, 2005]; transmission-line networks [*Alitalo et al.*, 2008]; parallel-plate [*Alitalo and Tretyakov*, 2010], and metamaterials [*Ni et al.*, 2015]. Unfortunately, all such approaches suffer from several drawbacks: they are dependent on the geometry and shape of objects to cloak, not suited for electrically large dimensions, relying on material properties not easily found in nature and extremely sensitive to material losses and polarization changes.

The aim of this work is to present a general approach for designing devices able to control and tailor electromagnetic surface waves for both amplitude and phase. First, an analytical model is derived to describe the surface wave propagation properties in terms of amplitude and phase (section 2), providing a detailed description of the field configurations. Then, by exploiting such analysis, the design procedure will be reported (section 3), giving us more physical insights onto the electromagnetic characteristics of the structure. Finally, to validate both the model and design steps, a practical realization for surface wave cloaking has been developed (section 4): three different samples (flat plane, uncloaked, and cloaked object) have been compared. The device shows good performances in reconstructing properly the wavefronts for both amplitude and phase.

2. Surface Wave Device Modeling

Dielectric slabs, with or without any associated metal, are used to contain the wave energy within a given space and guide it toward a specific direction. Usually, these are referred to as *dielectric waveguides*, and the field modes that they can support are known as surface wave modes [*Richmond*, 1959]. To simplify the model, let us reduce the problem to a 2-D one by considering the width in the *x*-direction infinite, so that $\partial/\partial x = 0$. Even though the dimensions of the structure are finite in practice, the two-dimensional (2-D) approximation not only simplifies the model but also gives us in-depth physical insights of surface wave propagation. We also assume that the waves are traveling in the $\pm z$ directions, which are infinite. Inside the dielectric slab waveguide, waves bounce back and forth between its upper and lower interfaces at an incidence angle greater than its critical angle. When this is accomplished, refracted fields outside the dielectric slab form evanescent (decaying) waves. These characteristics can be analyzed by treating it as a boundary-value problem (modal analysis) and/or by using geometrical optics (ray-tracing). Since we are interest in controlling both amplitude and phase wave properties of electromagnetic waves, we will apply both: the first approach to solve relevant wave equations satisfying prescribed boundary conditions and the second method to model the phase propagation of the wave along the structure.

2.1. Dielectric Slab Waveguide With the Ground: Field Configurations

Before starting to model the structure of interest, we analyze the wave behavior in terms of electric and magnetic field distributions in a traditional dielectric slab, as shown in Figure 1a. Typically, the cross section of the slab would be rectangular with height *h* and finite width *a*. According to *Zahn* [1979], the transverse magnetic to the *z* direction (TM_z) (transverse electric (TE)) mode fields that can exist within and outside the dielectric slab must satisfy

$$\nabla^2 P_z(x,y,z) + \beta^2 \cdot P_z(x,y,z) = 0 \tag{1}$$

being P_z the potential function representing the fields either within or outside the dielectric slab.

The solution is obtained by using the separation-of-variables method [*Collin*, 1960], according to the given geometry and associated boundary conditions. More specifically, within the dielectric slab the potential function P_z takes the following form [*Marcuvitz*, 1951]:

$$P_z(x,y,z) = A_d \left[B_d \cos\left(\beta_{yd}y\right) + C_d \sin\left(\beta_{yd}y\right) \right] e^{-j\beta_z z} \tag{2}$$

For the slab to function as a waveguide, the fields outside the dielectric slab must be of evanescent form. Therefore, outside the slab we have [*Harrington*, 1961]

$$P_z(x,y,z) = A_o \left[B_o e^{-j\beta_{yo}y} + C_o e^{-j\beta_{yo}y} \right] e^{-j\beta_z z} \tag{3}$$

with $\beta_{yd}^2 + \beta_z^2 = \beta_d^2 = \omega^2 \mu_d \varepsilon_d$ and $\beta_{y0}^2 + \beta_z^2 = -\alpha_{y0}^2 + \beta_z^2 = \omega^2 \mu_0 \varepsilon_0$ as the wave numbers within and outside the dielectric slab, respectively; A_i, B_i, and C_i are constants determined by the specific boundary conditions (*i* stays for: *d* as dielectric or 0 as air).

For a dielectric waveguide of height *h* with the ground plane as shown in Figure 1b, an additional boundary condition at *y* = 0 will be taken into the consideration: the vanishing of tangential electric components.
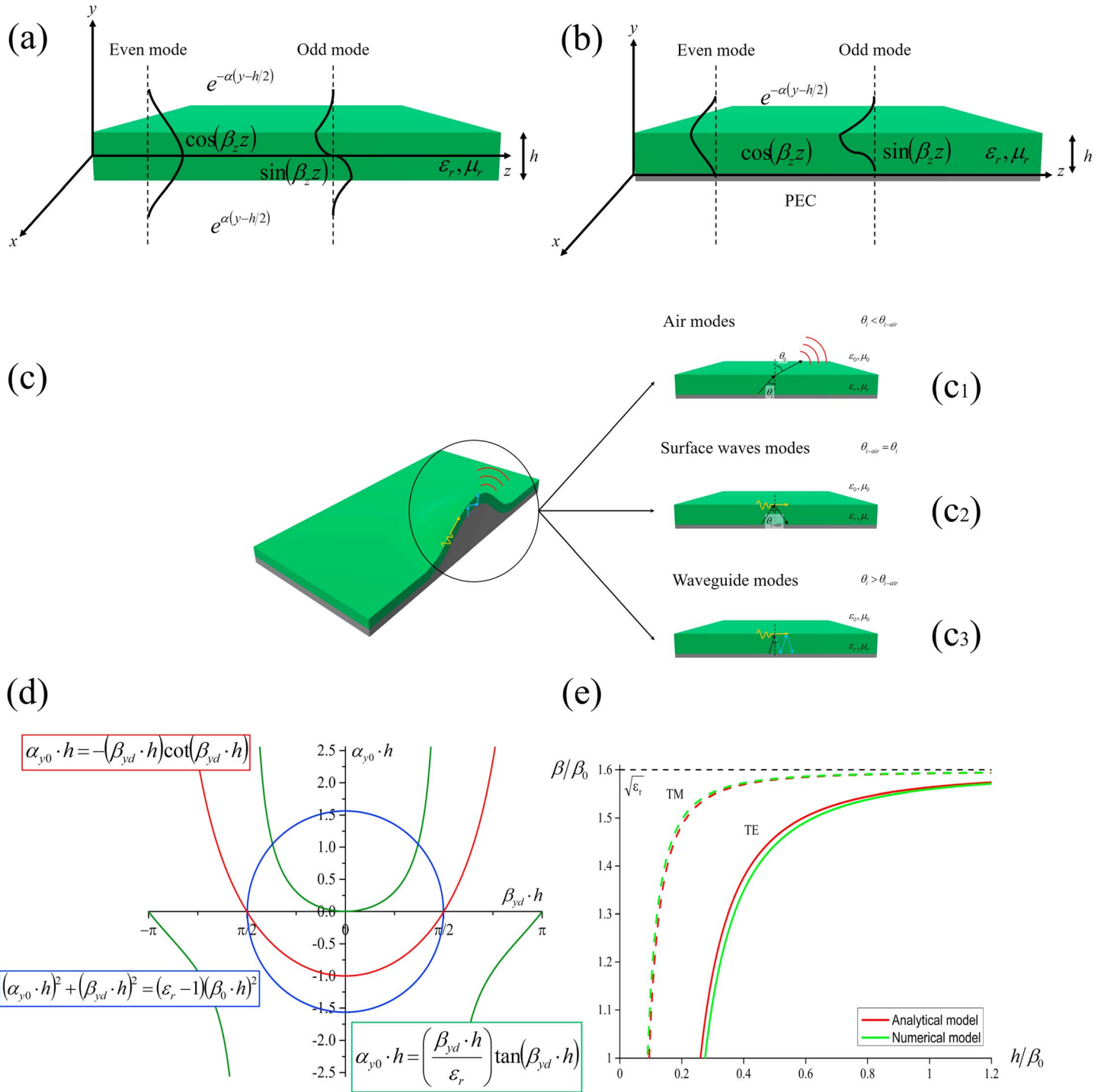
Figure 1. (a) Dielectric slab and (b) dielectric-covered ground plane waveguides: geometry (side-view) and even/odd mode field distributions. (c) Curvilinear grounded structure and propagating modes: air radiative waves (c₁), surface waves (c₂), and guided modes (c₃). (d) Graphical solution of the transcendental dispersion equation for the cutoff frequency of a TM (intersection green curve–blue curve) and TE (intersection red curve–blue curve) surface wave modes of the grounded dielectric sheet. (e) Surface wave propagation constants for the grounded dielectric slab: comparison of analytical model (closed-form formula) and numerical model of the dispersion equation.

Examining mathematical expressions (see detailed formulas in the supporting information) for both TE_z and TM_z, it is apparent that only tangential electric field components TM_z (odd) and TE_z (even) satisfy the boundary conditions and therefore supported by the proposed geometry [*Walter*, 1965].

2.2. Dielectric Slab Waveguide With the Ground: Phase Pattern

Let us assume that a curved slab is bounded above by air and below by the ground plane acting as perfect electric conductor (PEC), as shown in Figure 1c, such that $\varepsilon_r > \varepsilon_0$. The modal picture of waves in the proposed structure will be shown as the following:

1. Air modes: let us increase the incident angle θ_i gradually starting at $\theta_i = 0$. When θ_i is small, a wave that enters the slab will be reflected at the bottom from the PEC, refracted by the discontinuity at the slab-air interface, and will exit into the air provided that $\theta_i < \theta_{i\text{-air}}$. When the angle of incidence is smaller than the critical angles, the wave is transmitted to the air at an angle of $\theta_{i\text{-air}}$, greater than the incident angle θ_i. Electromagnetic waves are directed along the direction at the angle of refraction, θ_{air}. In this situation, waves propagate freely in the forms of *guided substrate* modes within the slab and *radiation* fields in the air, as shown in Figure 1c$_1$.

2. Surface wave modes: as the angle of incidence θ_i increases and reaches the critical angle $\theta_i = \theta_{i\text{-air}}$, the refracted angle θ_{air} varies more rapidly than the incident angle θ_i, and eventually reaches at 90°. Electromagnetic waves are evanescent, which travel along the *z* axis (parallel to the interface), while the constant phase planes are parallel to the *x* axis. There will be no real power transferred normal to the boundary from the dielectric slab into the air. Such waves take the name of *loosely* bound *surface wave*, as shown in Figure 1c$_2$.

3. Waveguide modes: When θ_i increases such that it passes the critical angle $\theta_{i\text{-air}}$ of the grounded dielectric slab/air interface, the wave is totally reflected at the slab/air interface. This describes a situation similar to the case B. The only difference is for the *surface wave*, traveling parallel to the interface (*z* axis) with a phase velocity that is less than that of an ordinary wave in the same medium, and it is rapidly attenuated in a direction normal to the interface (*x* direction) with an effective attenuation constant. This wave is referred to as a *tightly* bound *slow* surface wave.

Moreover, due to the presence of PEC underneath, for the *total reflection* effect at both upper and bottom interfaces, electromagnetic waves are totally reflected at both interfaces; in this case, we refer to electric and magnetic fields as *guided* modes, as shown in Figure 1c$_3$. For these modes, the energy is trapped within the dielectric slab and diverted toward a given direction. Specifically, the fact that horizontal wave vector components are equal indicates that electromagnetic waves propagate at a constant velocity in the *z* direction, assuming that the thickness of dielectric slab is much smaller than the operating wavelength.

The distinction between electromagnetic surface and guided waves is generally evaluated by considering two main aspects: excitation/source and the medium supporting their propagation. In terms of source, for guided waves to maximize the energy transfer between the source and the material, very simple techniques can be exploited [*Mahmoud*, 1991]: the use of an iris or hole, a linear (loop) antenna oriented parallel (perpendicular) to the electric (magnetic) field lines in the waveguide, or the proper excitation of currents matching those of the desired modes. Excitation of surface waves is not trivial; in fact, specific configurations should be used to properly excite them such as [*Cottam*, 1989] prism-coupled configuration, grating coupled, and waveguide-coupled configurations.

In terms of material used, for guided waves the simplest case is represented by a linear and homogeneous material (i.e., air or any lossless dielectric) that can be considered infinite extended in the propagation direction. Similar considerations can be done for more complicated structures such as uniaxial dielectrics or bianisotropic materials. On the contrary, an electromagnetic surface wave is the result of a discontinuity of at least two materials. It exists at the interface of two half spaces, each occupied by a different material; remove the interface by making the two partnering materials identical, and the surface wave vanishes. Moreover, there is no guarantee that at a specific frequency, a chosen pair of partnering materials will necessarily support the existence of a surface wave.

In general, the configuration of material in the direction normal to the interface (homogeneous, isotropic, and dielectric or bianisotropic and periodically nonhomogeneous) coupled with the possible sources leads to the existence of different surface waves at specified frequency ranges and propagating in specific directions, with different phase speed, attenuation rate, and field modes [*Goldstein and Maugin*, 2001]: surface plasmon-polaritons, Zenneck waves, Dyakonov waves, Tamm waves, and the most recent Dyakonov-Tamm waves.

3. Design of Surface Wave Devices

In the proposed surface wave designs, we assume that electric and magnetic fields satisfy the following boundary conditions:

$$
\begin{aligned}
&E_z(x, y = 0, z) = 0 \\
&E_z(x, y > 0, z) < \infty \\
&E_z^d(x, y = h, z) = E_z^o(x, y = h, z) \\
&H_z^d(x, y = h, z) = H_z^0(x, y = h, z)
\end{aligned}
\tag{4}
$$

By applying conditions (4), the governing equations for the geometry of Figure 1b for TM_z (odd) and TE_z (even) modes can be found [*Goldstone and Oliner*, 1959]:

$$
TM \quad \alpha_{y0} \cdot h = \left(\frac{\beta_{yd} \cdot h}{\varepsilon_r} \right) \tan\left(\beta_{yd} \cdot h \right)
\tag{5.1}
$$

$$
TE \quad \alpha_{y0} \cdot h = -\left(\beta_{yd} \cdot h \right) \cot\left(\beta_{yd} \cdot h \right)
\tag{5.2}
$$

$$
\left(\alpha_{y0} \cdot h \right)^2 + \left(\beta_{yd} \cdot h \right)^2 = (\varepsilon_r - 1)(\beta_0 \cdot h)^2
\tag{5.3}
$$

A detailed mathematical derivation is present in the supporting information. Now that the TM_z^m (even) and TM_z^m (odd) modes and the corresponding *dispersion equation* have been determined, the next step is to find β_{yd}, α_{y0}, and β_z. This is accomplished by solving the transcendental (5.1) by using numerically or graphically techniques. Equation (5.3) represents a circle in the $\beta_{yd}h$-$\alpha_{y0}h$ plane, as shown in Figure 1d. The radius of the circle is $\sqrt{\varepsilon_r - 1}\beta_0 h$, which is proportional to the electrical thickness of the dielectric sheet. Equation (5.1) is also plotted in Figure 1d. The intersection of these curves implies a solution to both (5.1). As $\sqrt{\varepsilon_r - 1}\beta_0 h$ becomes larger, the circle may intersect more than one branch of equation (5.1), implying that more than one TM mode can propagate. For any nonzero thickness sheet with a relative permittivity greater than unity, there is at least one propagating TM mode, which we will call the fundamental (or dominant) TM_0 mode, with a zero-cutoff frequency. This means that the TM_0 mode will always propagate unattenuated no matter what the frequency of operation. From Figure 1d the next TM mode, the TM_1 mode, will not begin to propagate unless the radius of the circle becomes greater than π. Once β_{yd} and α_{y0} have been found for a surface wave mode, the field expressions can be found consequently. A similar procedure can be developed for TE modes.

Solution methods from transcendental equation obtained by graphical and/or numerical approaches are approximate. Alternatively, simple analytical closed-form formulas for the first fundamental modes can be found. Let us start from ((5.1)) and ((5.2)) and define $x = \beta_{yd}h$ and $y = \alpha_{y0}h$ in the range of interest ($-\pi \leq x \leq \pi$). The following identities can be applied to simplify equations (5.1):

$$
\begin{aligned}
x \tan(x) &= x^2 \frac{(\pi^2 - x^2)}{(\pi^2 - 4x^2)} \\
-x \cot(x) &= -\frac{(\pi^2 - 4x^2)}{(\pi^2 - x^2)}
\end{aligned}
\tag{6}
$$

In this way, it is possible to solve analytically the equation systems ((5.1)) to find out rigorously the wave numbers β_{yd} and α_{y0}:

$$
\begin{aligned}
TM &\begin{cases} y = \dfrac{x^2 \, (\pi^2 - x^2)}{\varepsilon_r \, (\pi^2 - 4x^2)} \\[2mm] x^2 + y^2 = (\varepsilon_r - 1)(k_0 d)^2 \end{cases} \\[4mm]
TE &\begin{cases} y = -\dfrac{(\pi^2 - 4x^2)}{(\pi^2 - x^2)} \\[2mm] x^2 + y^2 = (\varepsilon_r - 1)(k_0 d)^2 \end{cases}
\end{aligned}
\tag{7}
$$

The design procedure permits us to establish a relationship between the propagation characteristics of surface waves along the grounded dielectric slab and the geometrical/electromagnetic properties of the medium. To validate the approach, the relationship between the normalized wave number β_z/β_0 and dielectric

thickness h/λ_0 is evaluated for TE and TM modes. A comparison between the proposed analytical model and the classical numerical method [*Balanis*, 1982] is shown in Figure 1e. Good agreement is obtained. With such a procedure, it is clear what must be done to limit the number of unattenuated modes that can be supported by the structure and how their characteristics can be manipulated. The proposed approach is crucial to the design of any surface wave devices in according with specific requirements.

4. All-Dielectric Device for Controlling Surface Wave

4.1. Realization of the Surface Wave Cloak

To validate the aforementioned analytical model and design approach, we demonstrate how to realize a surface wave cloak with inhomogeneous dielectric profiles. The device shall be able to tailor electromagnetic propagation characteristics of any curved surface to emulate those of a flat one, in terms of both amplitude and phase. In addition, we apply the theory of transformation optics [*Pendry et al*., 2006; *Leonhardt*, 2006] to link the geometry, material profiles, and the control of electromagnetic waves altogether. The required permittivity profile is evaluated by equating the optical path, crossing the flat plane with homogeneous permittivity, to the one on the curved surface with inhomogeneous materials, in particular, for two orthogonal paths: the circular (of fixed radius, red) and the radial one (of fixed angle, blue) [*Mitchell-Thomas et al*., 2013], as shown in Figure 2a. See detailed formulas in the supporting information.

To physically realize such a profile, a discretization process has been performed on the continuous distribution to get a simple seven-layered structure, each of them with a specific dielectric value. In this way, both the surface and the dielectric slab have linear boundaries, and we can treat each layer with a constant thickness perpendicular to the surface of the metallic ground plane, as illustrated in Figure 2b. We use the modal approach (section 2.1) to evaluate the permittivity of the graded-index material: our aim is to bound as much as possible the electromagnetic field along the structure, to ensure minimal radiation from the surface when curved surfaces are implemented, and to simplify future manufacturing processes [*La Spada et al*., 2016]. So by solving the following equations equation (7), the total permittivity profile has been chosen in the range of 9–15: higher permittivity values are present at the bottom ($\varepsilon_r = 15$), gradually decreasing when the height of the object increases ($\varepsilon_r = 9$).

4.2. Results and Discussion

The structure under study consists of a metallic curved object, underneath a dielectric bump, above a ground plane. The device is illuminated by a horn antenna placed at the left, operating in the frequency range of our interest (Figure 2c). An absorbing layer is used to bound the entire structure in the x-y plane. Three different samples are considered: a flat dielectric slab with homogeneous permittivity used as a reference (Figure 2d$_1$), the 3-D metallic object with a uniform permittivity distribution (Figure 2d$_2$), and the object with the manufactured cloaking (Figure 2d$_3$).

The device has been studied and designed both analytically [*Wolfram Research, Inc*, 2014] and numerically by using a full-wave electromagnetic solver [*CST STUDIO SUITETM*, 2014]. In the evaluation, all materials are considered real-life devices, therefore with specific thickness and complex permittivity values (in terms of real and imaginary part). Here a spectral analysis has been used to decompose the complex signals into simpler parts by applying Fourier transform [*McManus et al*., 2016]. In our case, the electromagnetic wave (signal) in the spatial domain mainly consists of free-space and surface wave. Figure 3 shows the electric field component, perpendicular to the surface of the structure: 3-D scanning (Figure 3, left column), magnitude (Figure 3, middle column), and phase (Figure 3, right column). Here we consider only the E_z component instead of the full-field representation, since preliminary analytical and numerical analyses revealed that the other electric field components (along x and y) can be considered negligible compared to E_z (see detailed mathematical explanation in the supporting information). The distance is measured along a line (of distance d) after the metallic object to the end of the structure (forward scattering region). The frequency range of interest is 8–12 GHz, where the horn antenna source operates. Figure 3a illustrates the undisturbed field along the flat case. The flat sample case can be considered as a reference system to evaluate the device's cloaking performance, since the related electric and magnetic field configurations are well known and established in literature [*Moon and Spencer*, 1963]. Figure 3b shows perturbation in the electric field of the surface wave when a uniform dielectric is implemented. We note a large amount of forward surface wave scattering due to the
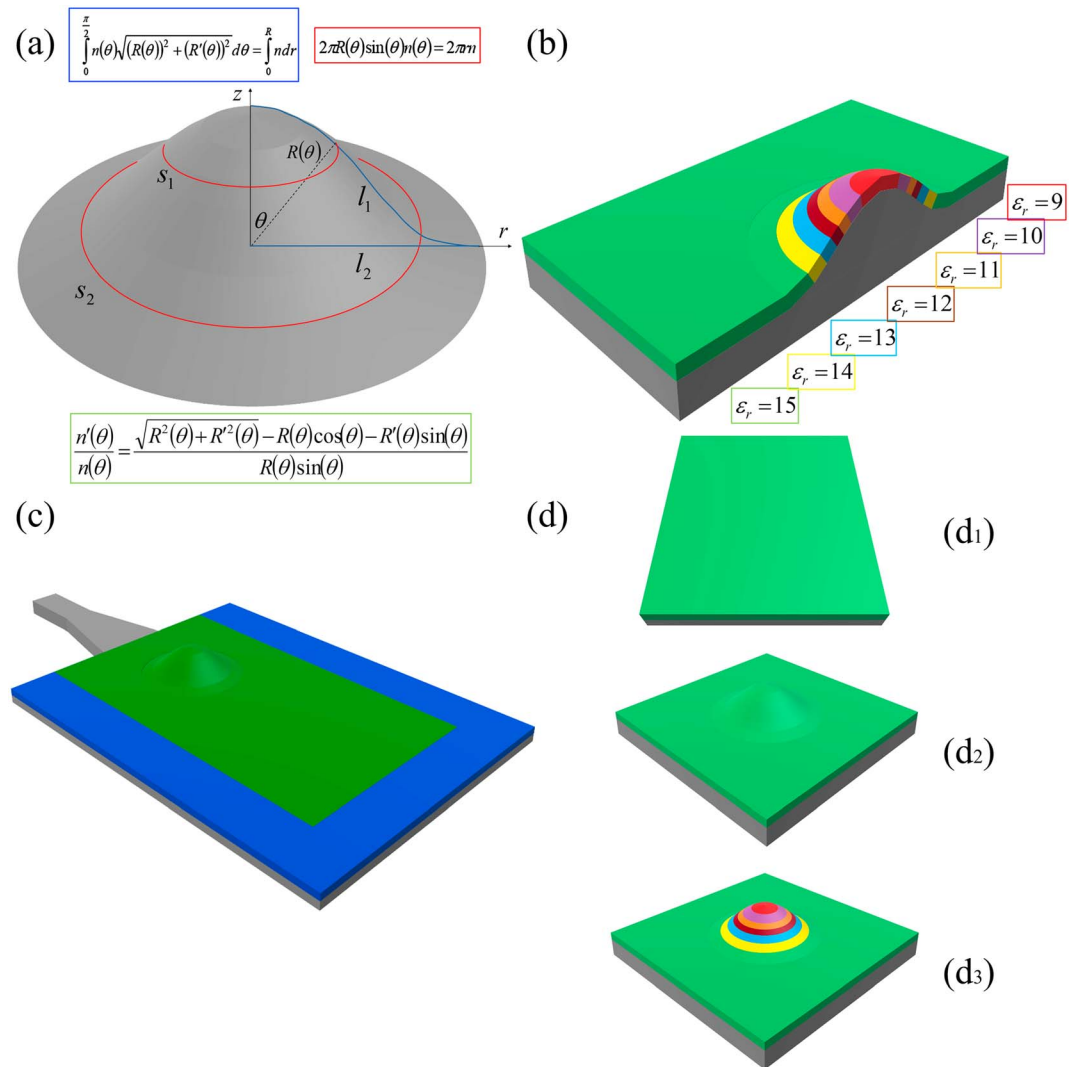
Figure 2. (a) Transformation optics principle: the picture illustrates the orthogonal raypaths in the curved space and flat space: radial geometric path lengths (blue lines), l_1 and l_2 respectively; circular geometric paths (red circles), s_1 and s_2, respectively. (b) Appropriate permittivity profile used to cloak the considered surface: radial cross section of the permittivity distribution, discretized in seven distinct dielectric layers. (c) Numerical setup used: the device is illuminated by an E-plane pyramid horn antenna in the frequency range of 8–12 GHz. An absorbing layer ($\varepsilon_r = 3.8$–$j7.2$) is used to bound the entire structure in the x-y plane. (d) Samples evaluated: flat plane, $\varepsilon_r = 15$ (d₁); uniform dielectric curved surface, $\varepsilon_r = 15$ (d₂); and graded-index distribution (d₃). All the three samples have equivalent planar dimensions (140 mm × 140 mm) and dielectric layer thickness (4.5 mm). The two samples containing the 3-D surface have height equal to 17.1 mm.

creation of destructive interference patterns (the shadow region). Such interferences can be attributed to the nonperfect coupling of the field along the structure, and the wave encounters the transitions flat-curved-flat. This phenomenon is observed particularly not only in the phase (right) but also in the amplitude (center). The magnitude of the scattered field is not too pronounced. In addition, it is visibly clear that the scattered amplitude does not follow the pattern of the flat plane and furthermore also decreases more rapidly than the reference surface wave. Figure 3c, shows the cloaking in action: the impinging wave from the left side is perfectly reconstructed on the right one. The surface wave is guided completely on the interface with no shadow left behind, as the obstacle is cloaked. Here it is clear that the cloak greatly reduces the amount of both backward and forward scattering for almost all frequencies considered in the range for both amplitude and phase. Although the surface wave device was designed to operate at 10 GHz, this work demonstrates a large bandwidth of operation where the performances are accurate in the reconstruction of the plane wavefronts: Figures 3d, 3e, and 3f for 8, 9, and 10 GHz, respectively.
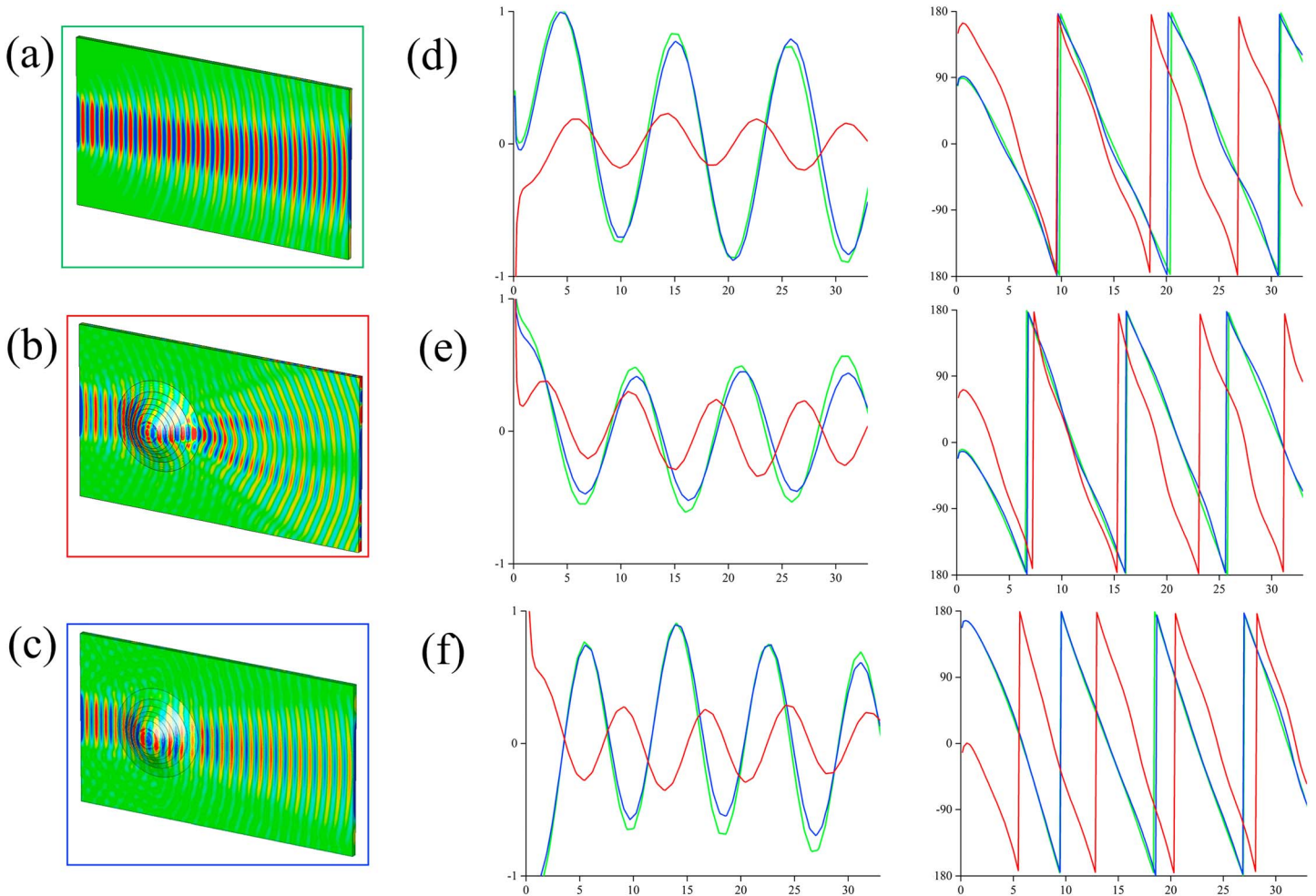
Figure 3. Normal component of the electric field along the dielectric slab surface, covering the curved metal object for all the three samples: (a) flat plane (reference), (b) uniform dielectric distribution, and (c) graded-index cloak. Amplitude (center) and phase (right) comparison at (d) 8 GHz, (e) 9 GHz, and (f) 10 GHz for flat plane sample (green), uniform dielectric distribution (red), and graded-index (blue) along a 30 mm sample line.

5. Conclusions

In this paper, a new modeling and design approach by combining transformation optics and modal analysis has been developed. It has been used to design devices with arbitrary geometries in order to freely manipulate and control electromagnetic surface waves on any surfaces. We have presented a generic approach, which can be scaled up for any frequency operations and mass production. To validate our approach, an all dielectric surface wave cloaking has been designed and simulated. Analytical and numerical results showed good performance and accuracy in restoring wavefronts in terms of both amplitude and phase. The sample device is insensitive to polarization changes and can operate within a wideband of frequencies. It is worth noting that such an approach is valid not only for electromagnetic waves, but it can also be applied to any wave-based phenomena, paving the way to a broader range of applications.

References

Alitalo, P., and S. A. Tretyakov (2010), Electromagnetic cloaking of strongly scattering cylindrical objects by a volumetric structure composed of conical metal plates, *Phys. Rev. B*, *82*(24) 245111.

Alitalo, P., O. Luukkonen, L. Jylha, J. Venermo, and S. A. Tretyakov (2008), Transmission-line networks cloaking objects from electromagnetic fields, *IEEE Trans. Antennas Propag.*, *56*(2), 416–424.

Balanis, C. A. (1982), *Antenna Theory: Analysis and Design*, 3rd ed., Wiley, Hoboken, N. J.

Chen, P.-Y., J. Soric, and A. Alù (2012), Invisibility and cloaking based on scattering cancellation, *Adv. Mater.*, *24*(44), 281–304.

Collin, R. E. (1960), *Field Theory of Guided Waves*, McGraw-Hill, New York.

Cottam, G. M. (1989), *Introduction to Surface and Superlattice Excitations*, Cambridge Univ. Press, New York.

CST STUDIO SUITETM (2014), CST of Europe, Inc.

Gill, A. E. (1982), Gravity wave, in *Atmosphere Ocean Dynamics*, pp. 247–311, Academic Press, Cambridge, England.

Goldstein, R. V. and G. A. Maugin (2001), *Surface Waves in Anisotropic and Laminated Bodies and Defects Detection*, NATO Sci. Ser. II, Dordrecht.

Goldstone, L. O., and A. A. Oliner (1959), Leaky wave antennas I: Rectangular waveguides, *IRE Trans. Antennas Propagat.*, *7*(4), 307–309.

Harrington, R. F. (1961), *Time-Harmonic Electromagnetic Fields*, McGraw-Hill, New York.

Hill, D. A., and J. R. Wait (1978), Excitation of the Zenneck surface wave by a vertical aperture, *Radio Sci.*, *13*(6), 969–977, doi:10.1029/RS013i006p00969.

Iovine, R., L. La Spada, and L. Vegni (2014), Optical properties of modified nanorod particles for biomedical sensing, *IEEE Trans. Magn.*, *50*(2), 169–172.

La Spada, L., and L. Vegni (2016), Metamaterial-based wideband electromagnetic wave absorber, *Opt. Express*, *24*(6), 5763–5772.

La Spada, L., T. M. McManus, A. Dyke, S. Haq, L. Zhang, Q. Cheng, and Y. Hao (2016), Surface wave cloak from graded refractive index nanocomposites, *Sci. Rep.*, *6*, 29363.

Leonhardt, U. (2006), Optical conformal mapping, *Science*, *312*(5781), 1777–1780.

Love, A. E. H. (1911), *Some Problems of Geodynamics*, Cambridge Univ. Press, Cambridge, England.

Mahmoud, F. (1991), *Electromagnetic Waveguides: Theory and Applications*, *IEE Electromagnetic Wave Ser.*, The IET, Stevenage, England.

Marcuvitz, N. (1951), *Waveguide Handbook*, McGraw-Hill, New York.

McManus, T. M., L. La Spada, and Y. Hao (2016), Isotropic and anisotropic surface wave cloaking techniques, *J. Opt.*, *18*(4) 044005.

Mitchell-Thomas, R. C., T. M. McManus, O. Quevedo-Teruel, S. A. R. Horsley, and Y. Hao (2013), Perfect surface wave cloaks, *Phys. Rev. Lett.*, *111*(21) 213901.

Moon, P., and D. E. Spencer (1963), *Field Theory Handbook*, Springer, Berlin.

Munk, B. A. (2005), *Frequency Selective Surfaces: Theory and Design*, John Wiley, Hoboken, N. J.

Ni, X., Z. J. Wong, M. Mrejen, Y. Wang, and X. Zhang (2015), An ultrathin invisibility skin cloak for visible light, *Science*, *349*(6254), 1310–1314.

Oliner, A. A. (1978), *Acoustic Surface Waves*, Springer, Berlin.

Pendry, J. B., D. Schurig, and D. R. Smith (2006), Controlling electromagnetic fields, *Science*, *312*(5781), 1780–1782.

Polo, J. A., T. G. Mackay, and A. Lakhtakia (2013), *Electromagnetic Surface Waves: A Modern Perspective*, Elsevier, London, U. K.

Richmond, J. H. (1959), *Reciprocity Theorems and Plane Surface Waves*, *Engineering Experiment Station Bulletin*, Ohio State Univ., Columbus.

Vegni, A. M., and V. Loscrì (2016), Characterization and performance analysis of a chiral-metamaterial channel with giant optical activity for terahertz communications, *Nano Commun. Networks*, *9*(1), 28–35.

Viktorov, I. A. (2013), *Rayleigh and Lamb Waves: Physical Theory and Applications*, Springer, New York.

Walter, C. H. (1965), *Traveling Wave Antennas*, McGraw-Hill, New York.

Wolfram Research, Inc (2014), *Mathematica, Version 10.0*, Champaign, Il.

Zahn, M. (1979), *Electromagnetic Field Theory*, John Wiley, New York.